

Hydrodynamic Characterization of a Column-type Prototype Bioreactor

Teodoro Espinosa-Solares · Marcos Morales-Contreras ·
Fabián Robles-Martínez · Melvin García-Nazariega ·
Consuelo Lobato-Calleros

Received: 8 May 2007 / Accepted: 30 November 2007 /
Published online: 3 January 2008
© Humana Press Inc. 2007

Abstract Agro-food industrial processes produce a large amount of residues, most of which are organic. One of the possible solutions for the treatment of these residues is anaerobic digestion in bioreactors. A novel 18-L bioreactor for treating waste water was designed based on pneumatic agitation and semispherical baffles. Flow patterns were visualized using the particle tracer technique. Circulation times were measured with the particle tracer and the thermal technique, while mixing times were measured using the thermal technique. Newtonian fluid and two non-Newtonian fluids were used to simulate the operational conditions. The results showed that the change from Newtonian to non-Newtonian properties reduces mixed zones and increases circulation and mixing times. Circulation time was similar when evaluated with the thermal and the tracer particle methods. It was possible to predict dimensionless mixing time (θ_m) using an equivalent Froude number (Fr_{eq}).

Keywords Flow pattern · Circulation time · Dimensionless mixing time · Froude number · Non-Newtonian behavior · Pneumatic agitation

Nomenclature

d_{eq} equivalent diameter (m)
 Fr_{eq} equivalent dimensionless Froude number (–)
 g gravitational acceleration ($m\ s^{-2}$)
 k consistency index ($Pa\ s^n$)

T. Espinosa-Solares · M. García-Nazariega
Departamento de Ingeniería Agroindustrial, Universidad Autónoma Chapingo, Apartado Postal no. 161,
Chapingo 56230 Estado de México, México

M. Morales-Contreras · F. Robles-Martínez
Unidad Profesional Interdisciplinaria de Biotecnología del Instituto Politécnico Nacional, México City,
DF, México

T. Espinosa-Solares (✉) · C. Lobato-Calleros
Posgrado en Ciencia y Tecnología Agroalimentaria, Universidad Autónoma Chapingo, Chapingo,
Estado de México, México
e-mail: espinosa@correo.chapingo.mx

n	flow behavior index (–)
R^2	coefficient of determination (–)
t_c	circulation time (s)
t_m	mixing time (s)
U_f	superficial velocity of the fluid (m s^{-1})
$\dot{\gamma}$	shear rate (s^{-1})
θ_m	dimensionless mixing time (–)
τ	shear stress (Pa)

Introduction

Biodigester design and operation for anaerobic digestion must usually balance hydrodynamic efficiency and microbial performance. While transport phenomena are improved by increasing the hydrodynamic conditions, excessive mixing could compromise the metabolic activity of the anaerobic consortia. Gómez et al. [1], working with anaerobic codigestion of primary sludge and the fruit and vegetable fraction of municipal solid wastes, reported that the absence of agitation resulted in a reduction in the specific gas production. In contrast, excess of shear force resulting from the digestate being passed through a pump or a mixer for long periods of time can disrupt the microbial communities dependent upon each other for fermentation. It has been reported by Shigematsu et al. [2] that mesophilic acetate-degrading methanogenic consortia modify their structure when the dilution rate is changed. Sheng et al. [3], studying the role of extracellular polymeric substances (EPS) on the stability of sludge flocs under shear conditions, demonstrated that external layers are easily dispersible by shear forces. This fact confirms the findings of Ong et al. [4] regarding the decrease in the production of EPS when excessive mixing was used during the cattle manure biomethanization. Espinosa-Solares et al. [5], working with chicken litter in a pilot plant anaerobic digester, reported that the poor consortia performance could be attributed to excessive mechanical work on the slurry; the fermentation mass was recycled six times in 24 h.

Several authors have reported a non-Newtonian behavior for anaerobic digestion media. Hashimoto and Chen [6], working with poultry waste slurries with 5.2% of total solids (TS), found a behavior flow index (n) of 0.28 and a consistency index (k) of 0.700 Pa s^n . Similar results were found by Chen [7] for beef-cattle manure; when the TS concentration was 6.2%, n and k were 0.73 and 0.070 Pa s^n , respectively. In the case of dairy cattle manure with 5.4% TS, Achkari-Begdouri and Goodrich [8] reported flow properties within the ranges of $0.69 \leq n \leq 0.77$ and $0.032 \leq k (\text{Pa s}^n) \leq 0.065$. For higher concentrations of dairy cattle manure (10% TS), the flow properties found by El-Mashad et al. [9] indicated a higher shear-thinning behavior ($0.31 \leq n \leq 0.34$; $10.5 \leq k (\text{Pa s}^n) \leq 13.0$) than the one found by Achkari-Begdouri and Goodrich [8]. To improve the performance of anaerobic digesters, flow properties have to be considered, particularly when a change in rheology is involved. Hydrodynamic characterization is a useful tool to define adequate performance of a bioreactor. Long-term operation geared toward a target efficiency of the bioreactor depends ultimately on the nature of the flow pattern obtained [10]. Espinosa-Solares et al. [11] studied flow patterns in stirred vessels using Newtonian and non-Newtonian fluids. These authors proposed a correlation between the dimensionless Froude number and the vortex length. This research group extended the previous study to assess dimensionless mixing time under different hydrodynamic conditions [12]. It was shown that rheological properties, gassing rate, and hydrodynamics played major roles in mixing time (t_m) when

the Froude number ranged from 0.40 to 0.71 and the dimensionless flow number varied from 0.00 to 0.06. Hence, mixing time is another key parameter for designing mixing systems. It has been defined by several authors as the time required to reach a specified degree of homogeneity [13, 14]. In fact, mixing time is a global index of mixing [15] and, consequently, the result of imposed hydrodynamics. As an initial approach for understanding the effect of mixing on anaerobic digestion, the hydrodynamics of a novel bioreactor was characterized. Thus, the aim of the present research was to study the mixing performance of this bioreactor, both qualitatively, via flow patterns, and quantitatively, using mixing and circulation times. The device was designed for wastewater treatment with both Newtonian and non-Newtonian model fluids, which mimic fermentation conditions. The column bioreactor includes semispherical baffles to improve aggregate retention in the bioreactor when the medium is mixed by pumping. The purpose of the top baffle is to promote mixing, while the bottom baffle is intended to favor sedimentation of large aggregates.

Materials and Methods

The novel bioreactor used was developed at the Instituto Politécnico Nacional. The column length is 1.152 m with an internal diameter of 0.144 m; it includes a draft tube (0.655 m high, 0.063 m inner diameter), two semispherical baffles, and a recirculation system. Figure 1 shows detailed measurements of the equipment. Fluid recirculation was achieved using a centrifugal pump (Little Giant, Oklahoma City, OK). The general flow starts when the fluid leaves the pump (marked as current 1 in Fig. 1) and enters the column, flowing through the draft tube. Once the fluid reaches the top baffle, part of the liquid goes downward, and the other could go upward. The fluid returns to the pump either through currents 2 and 3 (Fig. 1). Currents 4 and 5 are used, respectively, only during filling and flushing of the column reactor.

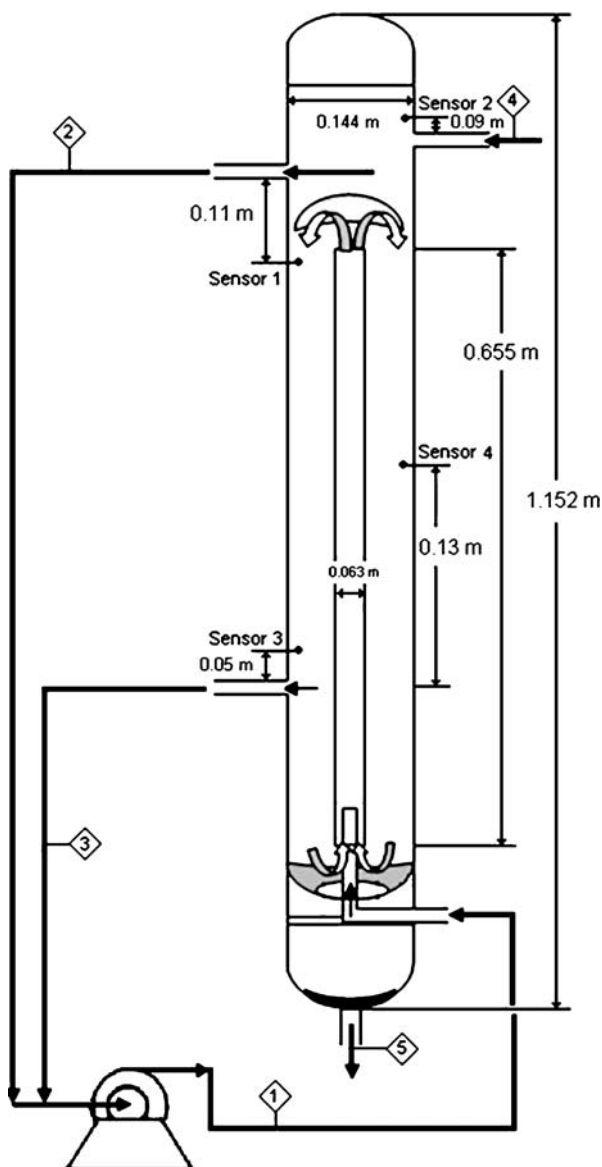
Experiments were conducted at room temperature. Water was used as the Newtonian fluid. Non-Newtonian liquids included aqueous solutions of Xanthan gum (Keltrol T, Kelco-Merck) as shear-thinning fluids. Solutions were prepared at constant ionic strength by adding 0.1% (w/v) NaCl. These fluids were selected because they had similar rheological properties to several anaerobic media [6–9] and they are clear fluids that allowed flow pattern visualizations.

The steady shear viscosity function was evaluated using a dynamic shear rheometer RHEOPLUS/32 V2.62 rheometer (Anton Paar, Messtechnik, Stuttgart, Germany) provided with cone-plate geometry, in which the rotating cone was 50 mm in diameter and cone angle was 1°. The viscosity for the shear-thinning fluids in the linear region was well fitted by the Ostwald–de Waele model (Eq. 1). The flow behavior index (n) of the non-Newtonian fluids varied from 0.34 to 0.53, the consistency index (k) between 0.086 and 0.637 Pa s ^{n} , and their density was 1,020 kg m⁻³. Deionized water was used throughout.

Flow patterns were visualized by adding tracer particles to the fluid, following the method reported by Espinosa-Solares et al. [11]. κ -Carrageenan particle tracers were introduced into the system through the recirculation tube at the top. A digital video camera was used to follow the particle trajectory through the bioreactor. The particle trajectory was drawn using bioreactor-scale sketches.

$$\tau = k \left(\dot{\gamma} \right)^n \quad (1)$$

Mixing time was determined using the thermal method reported by Espinosa-Solares et al. [12]. A small amount of the same working fluid at 40 °C above the working temperature was injected through the system pump. Mixing time was evaluated by means of the

Fig. 1 Experimental setup

evolution of fluid temperature distribution in the vessel after adding the thermal tracer. For that purpose, temperature changes in the vessel were measured by four thermocouples (k-type). The signals of the probes were acquired by an interface (model FDR98/061) from Pico Technology Limited (London, UK). Figure 1 shows the location of the thermocouples. Mixing is complete when uniform temperature distribution inside the tank is achieved [16]. Full details of the method were reported by Espinosa-Solares et al. [12]. Figure 2 shows the typical results of the thermal technique.

Circulation time (t_c) was evaluated using the particle tracers and the signals obtained by the thermal tests. For the tracers, circulation time was defined as the time required for the

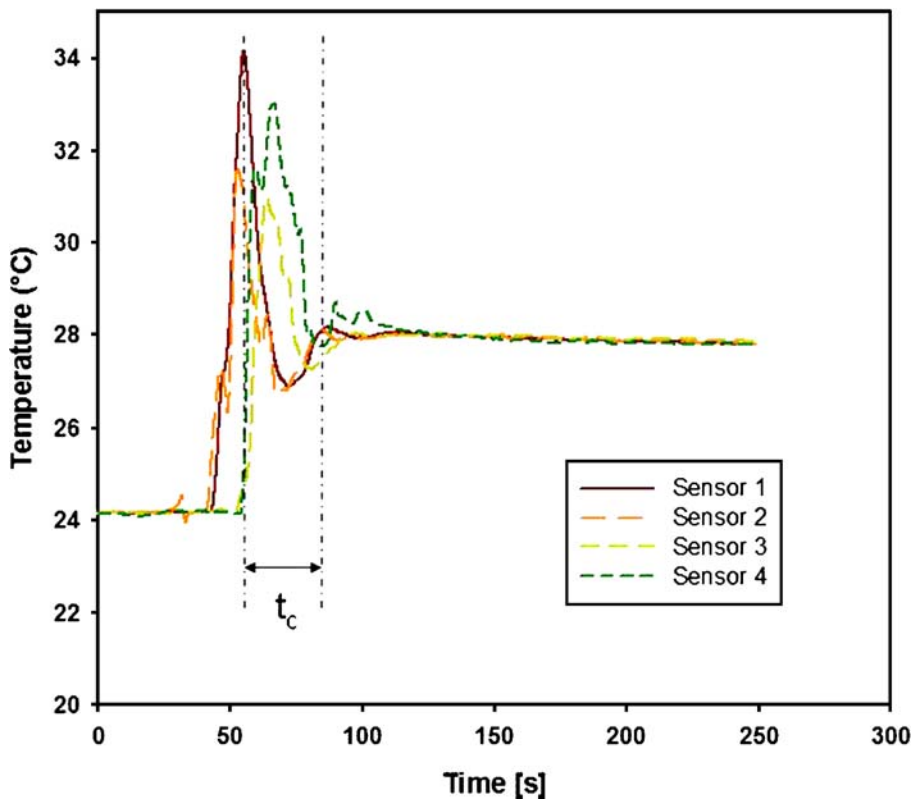


Fig. 2 Mixing time evaluation

particle to complete a circuit through the bioreactor. In the case of the thermal technique, circulation time was considered to be the time between first two consecutive peaks in the diagram obtained with the thermal method described previously. In all the cases, it was used only the signal of the sensor 1. Dimensionless mixing time was evaluated using mixing and circulation times obtained by the thermal method in the same manner as defined for airlift reactors [15]. Definition of the parameter is presented in Eq. 2, where θ_m represents the number of complete circuits needed in the bioreactor to achieve mixing. Dimensionless equivalent Froude number, Fr_{eq} , was evaluated with Eq. 3, where U_f , g , and d_{eq} represent fluid velocity, gravitational acceleration, and equivalent diameter of the annular section, respectively. The letter defined as the diameter of a circular section with the same area of the annular space; thus, the equivalent diameter enables the same flow rate as in the annular section.

$$\theta_m = \frac{t_m}{t_c} \quad (2)$$

$$Fr_{eq} = \frac{U_f^2}{g d_{eq}} \quad (3)$$

Results and Discussion

Flow Patterns

Figure 3 shows the flow patterns observed in the bioreactor using Newtonian (Fig. 3a, $n=1.00$, $k=0.001 \text{ Pa s}^n$) and two non-Newtonian fluids (Fig. 3b, $n=0.53$, $k=0.086 \text{ Pa s}^n$; Fig. 3c, $n=0.34$, $k=0.637 \text{ Pa s}^n$). It was found that the flow is generally similar, having pattern differences mainly in the draft tube and at the top section of the system. These differences depend on the rheological properties of the fluid. The fluid flows through the system beginning at the pump and continues to the bioreactor by the draft tube. When the fluid flows through the baffle at the top, it begins to flow down. Once the fluid reaches the exits marked 2 and 3 in Fig. 1, part of the fluid is suctioned into the pump input, while another part of the fluid continues flowing down to the semispherical baffle at the bottom of the bioreactor where it is incorporated into the flow imposed by the fluid coming from the pump.

The flow patterns that develop in different zones of the bioreactor are described as follows. Two patterns were observed in the draft tube; with the Newtonian fluid, as soon as the particle enters the draft tube until approximately 20 cm above the flow entrance, a rapid motion was observed. Passing this zone, the particle flows up in a straight line or in zigzag. In contrast, using non-Newtonian fluids, the particle movement is not so fast in the bottom 20 cm. This difference could be attributed to the smaller expected viscosity when the Newtonian fluid was used. After this point, the particles flow upward in a pattern similar to that obtained with the Newtonian fluid.

Agitation in the bioreactor is promoted mainly by the top baffle. In the Newtonian fluid, a well-defined zone of 16 cm, having small loops, was observed. In non-Newtonian fluids, these loops were occasionally observed. In this case, the top baffle improves the flow in the bioreactor in a manner similar to the helical flow promoter proposed by Wu and Merchuk [17].

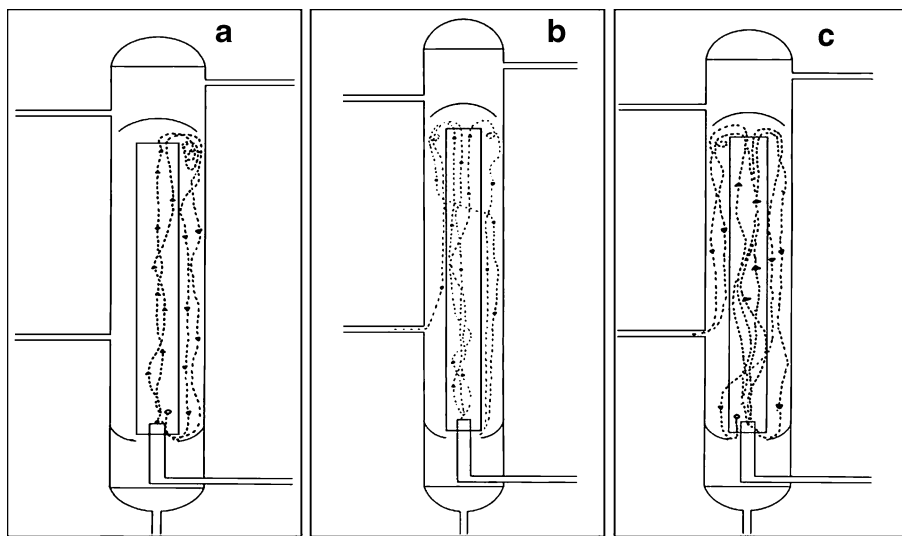


Fig. 3 Flow patterns using **a** Newtonian fluid (viscosity 1 mPa s) and two non-Newtonian fluids **b** $n=0.53$, $k=0.086 \text{ Pa s}^n$ and **c** $n=0.34$ and $k=0.637 \text{ Pa s}^n$

The flow in the annular section of the bioreactor is toward the baffle located at the bottom. The main flow is through the zone on the side opposite to the recirculation tubes. This flow pattern is more dominant in the Newtonian fluid (Fig. 3a), which could be attributed to the creation of a main flow where the particle is trapped. In all cases, the top baffle is important in keeping the particles within the body of the bioreactor. For the shear-thinning fluid with $n=0.53$ and $k=0.086 \text{ Pa s}^n$, it was detected that particles are slightly suctioned by the recirculation tube at the bottom of the bioreactor (Fig. 3b). This flow is more dominant with a higher shear-thinning fluid ($n=0.34$ and $k=0.637 \text{ Pa s}^n$, Fig. 3c).

Summarizing, the main recycling flow of the fluid, for a low-viscosity Newtonian fluid (0.001 Pa s), is from the draft tube to the vicinity of the top recirculation tube (indicated as 2 in Fig. 1). For non-Newtonian fluids with moderate shear-thinning behavior ($0.34 \leq n \leq 0.53$, and $0.034 \leq k \text{ (Pa s}^n\text{)} \leq 0.637$), the recycling flow is also from the draft tube to the vicinity of the recirculation top tube; however, the flow through the bottom recirculation tube (indicated as 3 in Fig. 1) becomes more important as shear thinning increases (Fig. 3b and c). The shear-thinning behavior of the fluids indicates that viscosity changes as shear rate does. Thus, according to the Ostwald–de Waele model presented in Eq. 1, for the non-Newtonian fluid with $n=0.53$ and $k=0.086 \text{ Pa s}^n$, viscosity changes from 0.010 to 0.040 Pa s when shear rate passes from 100 to 5 s^{-1} . In the case of another non-Newtonian fluid ($n=0.34$ and $k=0.637 \text{ Pa s}^n$), viscosity increases from 0.030 to 0.220 Pa s with the same shear rate variation. Thus, the increments in viscosity are, respectively, close to 410 and 720% . Any fluid dissipates energy while it flows because of viscosity forces. Thus, because no additional power is supplied along the flow pattern, it is expected a velocity reduction and consequently a decrement on shear rate as much as the fluid follows the path. The opposition to the flow at the bottom of the bioreactor in non-Newtonian fluids is attributed to the increment in the viscosity occasioned by a reduction in shear rate in that section of the bioreactor.

The baffle at the bottom has an apparently neutral effect on agitation; it does, however, allow particle separation. It was observed that particles with a mean weight of 0.01 g are incorporated into the flow described previously. At the same time, particles with a mean weight of 0.06 g settled. This section of the bioreactor should be adjusted to allow the separation of a specific particle size to satisfy specific needs, such as large sludge particles that could lose efficiency.

Circulation and Mixing Time

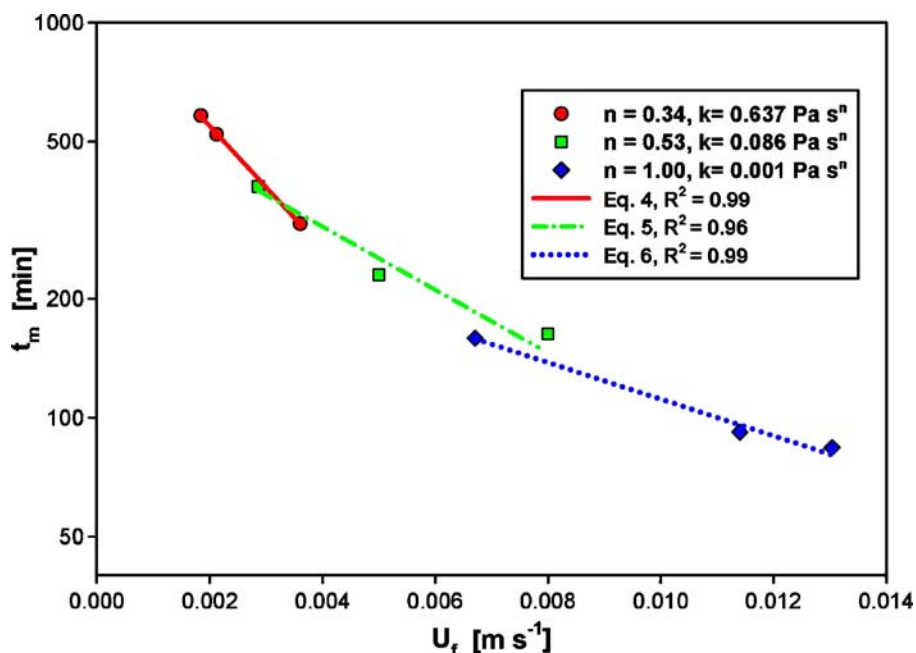
It was observed that hydrodynamics plays an important role in circulation time (Table 1). The increase in flow velocity reduces t_c . It is important to note in Table 1 that both techniques resulted in similar values for t_c for Newtonian and non-Newtonian fluids. Taking the t_c obtained by the tracer method as reference, the difference with t_c by thermal method ranges from 11 to 25% . Table 1 shows that t_c depends on flow properties; as flow index reduces, increasing at the same time the consistence index, t_c increases.

Figure 4 shows mixing time as a function of the fluid velocity. The effect of the increase in fluid velocity in reducing mixing time is expected. For example, for the fluid with highest shear-thinning behavior assessed here ($n=0.34$, $k=0.637 \text{ Pa s}^n$), when the velocity increases from 1.84×10^{-3} to $3.61 \times 10^{-3} \text{ m s}^{-1}$, mixing time decreases from 582 to 310 s . The reduction of mixing time by increasing velocity has been reported for draft tube airlift vessels by Gouveia et al. [18] and Sánchez Mirón et al. [15] using water as a working fluid. These research groups observed the trend with superficial aeration velocity below 0.045 and at 0.010 m s^{-1} , respectively. Mixing time in the bioreactor follows the exponential

Table 1 Circulation times for several hydrodynamic conditions.

U_f (m s ⁻¹)	n (–)	k (Pa s ^{<i>n</i>})	t_c tracer method (s)	t_c thermal method (s)
6.71×10^{-3}	1.00	0.001	24	27
1.14×10^{-2}	1.00	0.001	24	30
1.30×10^{-2}	1.00	0.001	37	33
2.86×10^{-3}	0.53	0.086	31	33
5.00×10^{-3}	0.53	0.086	36	38
8.00×10^{-3}	0.53	0.086	23	28
1.84×10^{-3}	0.34	0.637	44	47
2.12×10^{-3}	0.34	0.637	50	46

model presented in Eq. 4 ($R^2=0.99$). In a similar manner, Eqs. 5 ($R^2=0.96$) and 6 ($R^2=0.99$) describe mixing time as a function of the fluid, respectively, for another non-Newtonian fluid ($n=0.53$, $k=0.086$ Pa s^{*n*}) and the Newtonian one ($n=1.00$, $k=0.001$ Pa s^{*n*}). The exponential decreasing of mixing time by the increment in fluid velocity is notorious as the fluid increases the shear-thinning behavior. The influence of shear-thinning on t_m is possible to quantify by the values of the constant of the exponential term of the models presented in Eqs. 4 to 6. These findings have an important effect on the operation of the digester. For example, the poultry waste slurries ($n=0.28$, $k=0.700$ Pa s^{*n*}) reported by Hashimoto and Chen [6] will be expected to have higher mixing times and, at the same time, a higher influence on mixing time reduction than the beef-cattle manure ($n=0.73$, $k=$

**Fig. 4** Influence of velocity and flow behavior index on mixing time

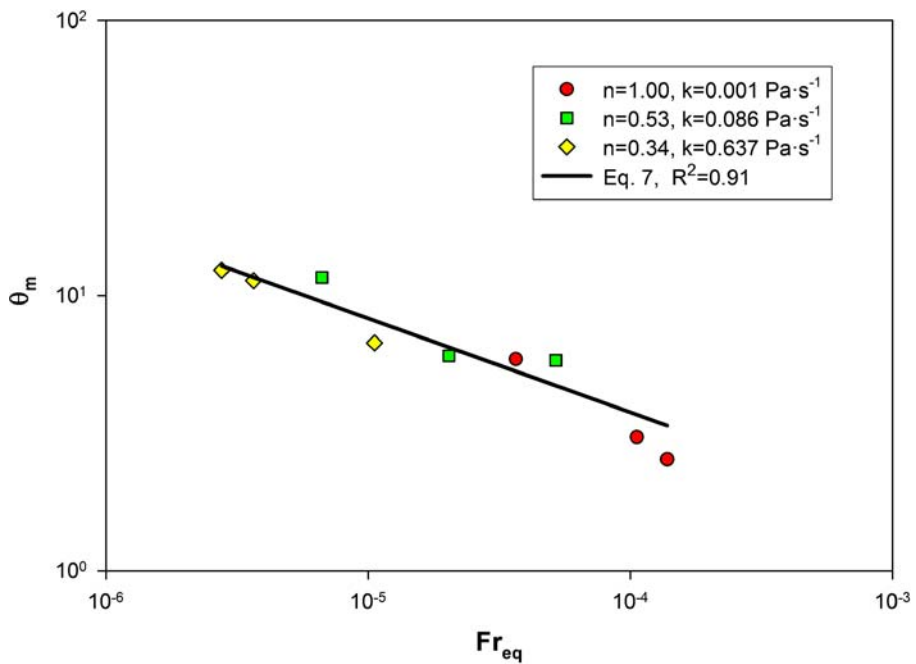


Fig. 5 Relationship between dimensionless mixing time and equivalent Froude number for the column type bioreactor

0.070 Pa sⁿ) referred by Chen [7]. Thus, for the latter, smaller energy requirements will be needed to achieve mixing.

$$t_m = 1119 e^{-357 U_f} \quad (4)$$

$$t_m = 636 e^{-184 U_f} \quad (5)$$

$$t_m = 324 e^{-107 U_f} \quad (6)$$

Dimensionless mixing time as a function of the Fr_{eq} is presented in Fig. 5 and Eq. 7. As can be observed, dimensionless mixing times for Newtonian and non-Newtonian fluids have the same trend. The model has a high coefficient of determination ($R^2=0.91$), suggesting that the Fr_{eq} is a parameter suitable for estimating dimensionless mixing regardless of the flow properties. The model indicates that by increasing the Fr_{eq} , a reduction in dimensionless mixing time is achieved, implying that a higher equivalent Froude number requires a fewer complete recycling circuits to achieve mixing. To illustrate this, under the operation conditions evaluated in this work, dimensionless mixing time was reduced from 12.4 to 2.5.

$$\theta_m = \frac{0.162}{Fr_{eq}^{0.34}} \quad (7)$$

Conclusions

The aim of the present work was to study the mixing performance of a novel bioreactor designed for wastewater treatment, using both Newtonian and non-Newtonian model fluids. The methodology included a blend of experimental techniques, such as flow visualization, and the evaluation of circulation and mixing times. The results showed that for the studied hydrodynamic conditions, main flow patterns are in general similar, having modifications depending on the rheological behavior of the fluids. Basically, two sections showed differences, the lower part of the draft tube and the vicinity of the top baffle. An increment in pseudoplasticity, which is related to a reduction in flow behavior index and, at the same time, to an increment in the consistence index, diminishes the mixed zones. The incorporation of a semispherical baffle at the top of the bioreactor favored agitation, while the baffle at the bottom favored particle settling. Under the operational conditions of the experiments ($Fr < 1.2 \times 10^{-4}$), Fr_{eq} has an inversely proportional relationship with dimensionless mixing time. These findings have interesting implications for bioreactor design and operation; for high shear-thinning media, higher energy requirements will be needed to increase the fluid velocity to achieve mixing. However, imposition of hydrodynamic conditions in the bioreactor could compromise mixing needs with microbial integrity, and so further work is needed to evaluate the influence of the hydrodynamic conditions on microbial performance, which is left for future communications.

Acknowledgments The authors gratefully acknowledge the financial support from Universidad Autónoma Chapingo and Instituto Politécnico Nacional. We would also like to acknowledge to Olga Lidia Martínez-Flores and Graciela Martínez-Ramírez for their contributions during the experimental work.

References

- Gómez, X., Cuertos, M. J., Cara, J., Morán, A., & García, A. I. (2006). *Renewable Energy*, 31, 2017–2024.
- Shigematsu, T., Tang, Y. Q., Kawaguchi, H., Ninomiya, K., Kijima, J., Kobayashi, T., Morimura, S., & Kida, K. (2003). *Journal of Bioscience and Bioengineering*, 96, 547–558.
- Sheng, G. P., Yu, H. Q., & Li, X. Y. (2006). *Biotechnology & Bioengineering*, 93, 1095–1102.
- Ong, H. K., Greenfield, P. F., & Pullammanappallil, P. C. (2002). *Environmental Technology*, 23, 1081–1090.
- Espinosa-Solares, T., Bombardiere, J., Domaschko, M., Chatfield, M., Stafford, D. A., Castillo-Angeles, S., et al. (2006). *Applied Biochemistry and Biotechnology*, 129–132, 959–968.
- Hashimoto, A. G., & Chen, Y. R. (1976). *Transactions of the ASAE*, 19, 930–934.
- Chen, R. Y. (1981). *Transactions of the ASAE*, 24, 187–192.
- Achkari-Begdouri, A., & Goodrich, P. R. (1992). *Bioresource Technology*, 40, 149–156.
- El-Mashad, H. M., van Loon, W. K. P., Zeeman, G., & Bot, G. P. A. (2005). *Bioresource Technology*, 96 (5), 531–535.
- Vesvikar, M. S., & Al-Dahhan, M. (2005). *Biotechnology and Bioengineering*, 89, 719–732.
- Espinosa-Solares, T., Brito de la Fuente, E., Tecante, A., & Tanguy, P. A. (2001). *Chemical Engineering & Technology*, 24, 913–918.
- Espinosa-Solares, T., Brito de la Fuente, E., Tecante, A., Medina-Torres, L., & Tanguy, P. A. (2002). *Chemical Engineering Research & Design*, 80, 817–823.
- Ulbrecht, J. (1974). *Chemical Engineering (London)*, pp. 347–353.
- Rzyski, E. (1993). *Chemical Engineering and Technology*, 16, 229–233.
- Sánchez Mirón, A., Cerón García, M.-C., García Camacho, F., Molina-Grima, E., & Chisti, Y. (2004). *Chemical Engineering Research & Design*, 82, 1367–1374.
- Ford, D. E., Mashelkar, R. A., & Ulbrecht, J. (1972). *Process Technology International*, 17, 10.
- Wu, X., & Merchuk, J. C. (2003). *Chemical Engineering Science*, 58, 1599–1614.
- Gouveia, E. R., Hokka, C. O., & Badino-Jr, A. C. (2003). *Brazilian Journal of Chemical Engineering*, 20, 363–374.